

# Production of multiply charged ion target for photoionization studies using synchrotron radiation in the soft x-ray region

Masaki OURA and Hitoshi YAMAOKA

Harima Institute, The Institute of Physical and Chemical Research (RIKEN),  
Mihara 323-3, Mikazuki-cho, Sayo-gun, Hyogo 679-5143, Japan

## 1. Introduction

Photoabsorption by positive ions is universal process in the radiative field accompanying high temperature plasmas such as fusion and astrophysical plasmas. Some theoretical works for photoionization of positive ions along the isonuclear sequence using the simple Hartree-Slater (HS) central-field model have stressed from those systematic studies that removal of outer-shell electrons have essentially no effect on inner-shell photoionization cross sections, except for a shift of threshold [1-3]. Further sophisticated calculations using the relativistic-random-phase approximation (RRPA) have been performed and the results support such earlier predictions [4]. On the other hand, concerning the isoelectronic sequence, as the nuclear charge  $Z$  is increased while the electron number remains the same, the central potential of the nucleus on each electron,  $-Ze^2/r_i$ , will increase in size relative to the noncentral interelectron potential,  $e^2/r_{ij}$ . This will give rise to a prediction improving accuracy of the central-potential calculation for ionic photoionization in going along the isoelectronic sequence [5]. These predictions have not, however, been experimentally confirmed so far. Furthermore, although the basic information on positive ions (especially on multiply charged ions, MCI), such as binding energies and photoionization/photoexcitation cross sections of each subshells, is important in various plasma applications, experimental study is scarce because of the difficulties in obtaining the dense ion target and the intensive monochromatic light.

Recent progress in the synchrotron radiation facility has made an appearance of the intense undulator radiation possible. This appearance has potential to overcome one of the difficulties mentioned above. In order to achieve the dense ion target, we have developed a photon-ion merged-beam apparatus [6] based on the experience established during the R&D program [7]. This apparatus can produce various ionic species as the MCI target by employing an electron cyclotron resonance ion source (ECRIS). In this report, we

describe the characteristics of the apparatus and discuss about potential use in measuring the photoionization cross sections.

## 2. Transport System of the MCI Beam

Main components of the apparatus are the ECRIS, the charge-selecting magnet, the interaction region and the cylindrical mirror analyzer (CMA) equipped with the position sensitive detector for product ions. Ions produced in the ECRIS are accelerated by the extraction voltage of 10 kV and are focused onto the entrance slits of the charge-selecting magnet by the first Einzel lens. The specific ions in the primary beam are selected and deflected 90 degrees by the magnet. Fig.1 shows a typical MCI spectrum, in which the ECRIS is optimized to achieve maximum intensity of  $\text{Ar}^{2+}$  and the RF power of 6 W is introduced into the plasma chamber, measured at the diagnostic Faraday cup mounted between the second beam-defining slits and the collimator. The mass-selected MCI beam is focused onto the collimator, consisting of a pair of 2 mm  $\phi$  orifices (100 mm apart), by the second Einzel lens. This collimator defines the ion beam size and divergence before it enters the interaction region. The interaction region, whose length is 120 mm, is floated to a certain voltage, normally at

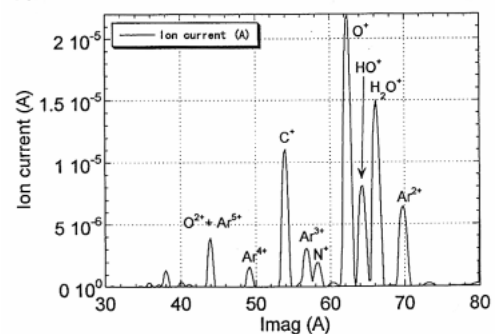


Figure 1. MCI spectrum measured at the diagnostic Faraday cup. Beam transport system was optimized to maximize the intensity of  $\text{Ar}^{2+}$ .

8 kV, so that the MCI beam suffers a deceleration when it enters, and accelerates again at the exit. Therefore the product ions will have the excess of the kinetic energy  $(q' - q)V_b$  corresponding to its charge state, where  $q'$  is the charge state of the product ions,  $q$  the charge of the primary ions and  $V_b$  the voltage applied to the interaction region. The MCI beam passing through the interaction region and the product ions enter the CMA and take orbits corresponding to the ratio  $E/q'$ , where  $E$  is the total kinetic energy. The beam current of  $Ar^{2+}$  at the Faraday cup settled at the CMA was measured to be about 420 enA. By changing the magnet setup, the beam current of several ionic species have been measured and the results are summarized in Table 1. We should notice that the RF input is suppressed to be less than 10 W because the apparatus is under its early commissioning phase. An operation with maximum RF input (200 W) will soon be available and we will get more dense ion target.

### 3. Feasibility of photoionization experiment

For a photoabsorption (photoexcitation / photoionization) experiment by means of photoion yield spectroscopy with the present apparatus, the following photoion production rate can be expressed,

$$\frac{dN}{dt} = \sigma \phi \rho l F$$

where  $\sigma$  is the photoabsorption cross section ( $cm^2$ ),  $\phi$  the photon flux (photons/sec),  $\rho$  the ion target density ( $ions/cm^3$ ),  $l$  the interaction length (cm), and  $F$  the overlap integral of the synchrotron radiation and the ion target in the interaction region. Assuming ionization of

the 2p electron in  $Ar^{2+}$ , the following values apply:  $\sigma \sim 10^{-18} cm^2$  at 500 eV photon energy [8],  $\phi \sim 10^{12}$  photons/sec,  $\rho = 3 \times 10^6 ions/cm^3$ ,  $l = 12 cm$ , and  $F \sim 0.56$  (assuming a photon beam radius of 1.5 mm and ion beam radius of 2 mm). These values give a photoion production rate 20 ions/sec. As was mentioned above, present ion target density has been achieved with a poor RF input. We think we can expect the photoion production rate of several times as large as the present estimation.

### References

- [1] D. W. Missavage, S. T. Manson and G. R. Daum, Phys. Rev. **A15** (1977) 1001.
- [2] R. F. Reilman and S. T. Manson, Phys. Rev. **A18** (1978) 2124.
- [3] K. D. Chao and S. T. Manson, Phys. Rev. **A24** (1981) 2481.
- [4] G. Nasreen, S. T. Manson and P. C. Deshmukh, Phys. Rev. **A40** (1989) 6091.
- [5] A. Msezane, R. F. Reilman, S. T. Manson, J. R. Swanson and L. Armstrong, Jr., Phys. Rev. **A15** (1977) 668.
- [6] M. Oura et al., J. Synchrotron Rad. **5** (1998) 1058.
- [7] M. Oura et al., Nucl. Instrum. Methods **B86** (1994) 190.
- [8] D. A. Verner, D. G. Yakovlev, I. M. Band and M. B. Trzhaskovskaya, At. Data and Nucl. Data Tables **55** (1993) 233.

Table 1. Measured ion beam current and ion target density

Ionic species	Beam current		Current density (pA/mm <sup>2</sup> )	Ion target density (ions/cm <sup>3</sup> )
	(enA)	(pA)		
Ar <sup>+</sup>	340	340	108.2	6.9x10 <sup>6</sup>
Ar <sup>2+</sup>	420	170	66.8	3.0x10 <sup>6</sup>
Ar <sup>3+</sup>	340	113	36.1	1.3x10 <sup>6</sup>
Ar <sup>4+</sup>	180	45	14.3	4.6x10 <sup>5</sup>
O <sup>+</sup>	240	240	76.4	3.1x10 <sup>6</sup>
O <sup>3+</sup>	45	15	4.8	1.1x10 <sup>5</sup>